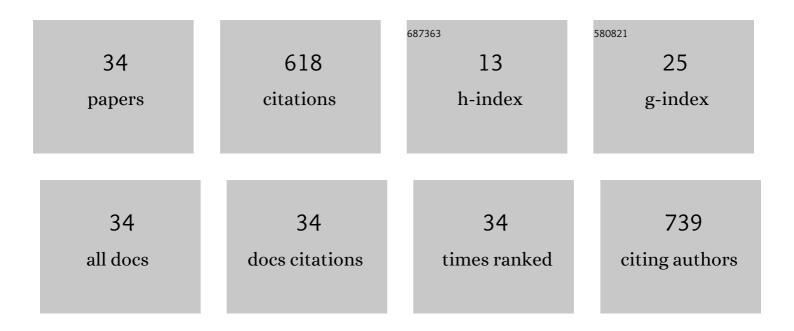
Hongkai Wang

List of Publications by Year in descending order

Source: https://exaly.com/author-pdf/11821726/publications.pdf Version: 2024-02-01



ΗΟΝΟΚΑΙ ΜΛΑΝΟ

#	Article	IF	CITATIONS
1	Reconstruction for free-space fluorescence tomography using a novel hybrid adaptive finite element algorithm. Optics Express, 2007, 15, 18300.	3.4	126
2	Ganoderma lucidum polysaccharide peptide prevents renal ischemia reperfusion injury via counteracting oxidative stress. Scientific Reports, 2015, 5, 16910.	3.3	74
3	The hidden cost of housing practices: using noninvasive imaging to quantify the metabolic demands of chronic cold stress of laboratory mice. Comparative Medicine, 2013, 63, 386-91.	1.0	51
4	In vivo x-ray luminescence tomographic imaging with single-view data. Optics Letters, 2013, 38, 4530.	3.3	49
5	Estimation of Mouse Organ Locations Through Registration of a Statistical Mouse Atlas With Micro-CT Images. IEEE Transactions on Medical Imaging, 2012, 31, 88-102.	8.9	47
6	High urea induces depression and LTP impairment through mTOR signalling suppression caused by carbamylation. EBioMedicine, 2019, 48, 478-490.	6.1	28
7	Urea. Sub-Cellular Biochemistry, 2014, 73, 7-29.	2.4	23
8	3D-SIFT-Flow for atlas-based CT liver image segmentation. Medical Physics, 2016, 43, 2229-2241.	3.0	20
9	A wavelet-based single-view reconstruction approach for cone beam x-ray luminescence tomography imaging. Biomedical Optics Express, 2014, 5, 3848.	2.9	18
10	MARS: a mouse atlas registration system based on a planar x-ray projector and an optical camera. Physics in Medicine and Biology, 2012, 57, 6063-6077.	3.0	17
11	A Deformable Atlas of the Laboratory Mouse. Molecular Imaging and Biology, 2015, 17, 18-28.	2.6	16
12	Excitation-resolved cone-beam x-ray luminescence tomography. Journal of Biomedical Optics, 2015, 20, 070501.	2.6	15
13	Mouse Atlas Registration with Non-tomographic Imaging Modalities—a Pilot Study Based on Simulation. Molecular Imaging and Biology, 2012, 14, 408-419.	2.6	13
14	Deformable torso phantoms of Chinese adults for personalized anatomy modelling. Journal of Anatomy, 2018, 233, 121-134.	1.5	13
15	Elevated urinary urea by high-protein diet could be one of the inducements of bladder disorders. Journal of Translational Medicine, 2016, 14, 53.	4.4	12
16	Water Transport Mediated by Other Membrane Proteins. Advances in Experimental Medicine and Biology, 2017, 969, 251-261.	1.6	12
17	A method of 2D/3D registration of a statistical mouse atlas with a planar X-ray projection and an optical photo. Medical Image Analysis, 2013, 17, 401-416.	11.6	11
18	Deformable Head Atlas of Chinese Adults Incorporating Inter-Subject Anatomical Variations. IEEE Access, 2018, 6, 51392-51400.	4.2	10

Hongkai Wang

#	Article	IF	CITATIONS
19	Bioluminescence tomography with structural information estimated via statistical mouse atlas registration. Biomedical Optics Express, 2018, 9, 3544.	2.9	9
20	Dual-modality multi-atlas segmentation of torso organs from [18F]FDG-PET/CT images. International Journal of Computer Assisted Radiology and Surgery, 2019, 14, 473-482.	2.8	9
21	Statistical Evaluation of Radiofrequency Exposure during Magnetic Resonant Imaging: Application of Whole-Body Individual Human Model and Body Motion in the Coil. International Journal of Environmental Research and Public Health, 2019, 16, 1069.	2.6	9
22	Serum metabolomics of end-stage renal disease patients with depression: potential biomarkers for diagnosis. Renal Failure, 2021, 43, 1479-1491.	2.1	7
23	Bioluminescence tomography reconstruction in conjunction with an organ probability map as an anatomical reference. Biomedical Optics Express, 2022, 13, 1275.	2.9	7
24	Expression of Urea Transporter B in Normal and Injured Brain. Frontiers in Neuroanatomy, 2021, 15, 591726.	1.7	5
25	Automated brain structures segmentation from PET/CT images based on landmark-constrained dual-modality atlas registration. Physics in Medicine and Biology, 2021, 66, 095003.	3.0	4
26	Abdominal atlas mapping in CT and MR volume images using a normalized abdominal coordinate system. Computerized Medical Imaging and Graphics, 2008, 32, 442-451.	5.8	3
27	Non-stationary reconstruction for dynamic fluorescence molecular tomography with extended kalman filter. Biomedical Optics Express, 2016, 7, 4527.	2.9	3
28	Inter-Subject Shape Correspondence Computation From Medical Images Without Organ Segmentation. IEEE Access, 2019, 7, 130772-130781.	4.2	2
29	Deformable Torso Anatomy Education with Three-Dimensional Autostereoscopic Visualization and Free-Hand Interaction. , 2022, , .		2
30	A Novel Merged Strategy with Deformation Field Reconstruction for Constructing Statistical Shape Models. , 2019, , .		1
31	Evaluation of different atlas selection strategies for multi-atlas segmentation of low-dose computed tomographic images of whole-body positron emission tomography/computed tomography. Digital Medicine, 2017, 3, 186.	0.1	1
32	A Statistical Model of Spine Shape and Material for Population-Oriented Biomechanical Simulation. IEEE Access, 2021, 9, 155805-155814.	4.2	1
33	Organ concentration quantification for small animal PET images by registration with a statistical mouse atlas. , 2010, , .		0
34	Nanobiomaterials in X-ray luminescence computed tomography (XLCT) imaging. , 2016, , 403-420.		0